Core modified *meso*-aryl sapphyrins and rubyrins: structural and anion receptor properties

Alagar Srinivasan,[a] Venkataramana Rao G. Anand,[a] Simi K. Pushpan,[a] Tavarekere K. Chandrashekar,*[a] Ken-ichi Sugiura[b] and Yoshiteru Sakata[b]

[a] *Department of Chemistry, Indian Institute of Technology, Kanpur, U. P. 208 016, India*
[b] *Institute of Scientific and Industrial Research, Osaka University, Osaka 567, Japan*

Received (in Cambridge, UK) 13th June 2000, Accepted 30th June 2000
Published on the Web 9th August 2000

Studies on structural characterisation and anion binding properties of a series of core modified *meso*-aryl sapphyrins and rubyrins are described. It has been shown that the sapphyrins and rubyrins bind anions such as F^-, N_3^- and CO_3^{2-} in their protonated form. The binding constants evaluated for a particular sapphyrin vary in the order $F^- \cong N_3^- < CO_3^{2-}$ and this has been accounted for in terms of compatibility of the cavity size of the sapphyrin, the anion size and the complete charge neutralisation. However, for the protonated rubyrins, this order is reversed because of the larger cavity sizes of the rubyrins relative to the sapphyrins. A comparison of the magnitude of binding constants with those of β-substituted N5 sapphyrins indicates a decrease of several orders of magnitude because of the availability of fewer hydrogen bonding sites for the core modified *meso*-aryl sapphyrins reported here. Furthermore, the single crystal X-ray structures of two sapphyrins reveal the inversion of the heterocyclic ring opposite to the bithiophene/biselenophene unit, while the rubyrins show planar structures.

Introduction

Sapphyrins and rubyrins are a class of expanded porphyrins containing 22 and 26 π electrons respectively in their molecular skeleton.[1] Compared to normal porphyrins, they have larger cavities, more π-electrons in conjugation and an increased number of heteroatoms (five for sapphyrins and six for rubyrins). Substitution of one or more nitrogens by other heteroatoms such as S, Se and O not only alters the cavity sizes but also affects the electronic structure and this is reflected in altered optical, electrochemical and photochemical properties.[2] Furthermore, the recent realisation that the expanded porphyrins in general have diverse applications in biomedical areas as photosensitisers,[3] MRI contrasting agents,[4] or radiation sensitisers[5] has increased research activity to exploit their diverse properties.

Because of the enhanced basicity of sapphyrins and rubyrins relative to porphyrins and the availability of larger cavities, they have the ability to coordinate anions, and in favourable cases even transport of anions using sapphyrins has been reported.[6] A large number of anion complexes of protonated sapphyrin **1** (Scheme 1) have been characterised by Sessler and coworkers both in solid and solution phases. It has been shown that the binding modes of anions depends on the compatibility of cavity size of the sapphyrin and the anion size.[7] The anion is found in the centre of the cavity of sapphyrin with five N–H···F hydrogen bonds in the F^- complex[8] while in the phosphate,[9] carboxylate[10] and azide complexes[11] of the protonated form of **1**, the anions are found above and below the mean sapphyrin plane and the anions are held by hydrogen bonds. In the chloride complex of protonated rubyrin **2**, the two chloride anions are sitting above and below the mean plane at a distance of 1.6 Å through six N–H···Cl bonds.[12] A recent report from this laboratory has shown that one trifluoroacetate anion binds to modified sapphyrins involving both carboxy and carbonyl oxygens through three N–H···O hydrogen bonds.[13] In continuation of our efforts in this direction, we have studied the anion binding characteristics of a series of sapphyrins **3**–**6** and rubyrins **7**–**10** (Scheme 1). Furthermore, the structures of two sapphyrins **4** and **6** have been determined by single crystal X-ray crystallography and they are found to have inverted structures where the heterocyclic ring opposite to the bithiophene/biselenophene unit is inverted. The details of these studies are reported in this paper.

Experimental

The syntheses and the spectroscopic characterisation of sapphyrins **3**–**6** and rubyrins **7**–**10** have been described in our earlier reports.[14,15] The crystals for the X-ray analysis of **4** and **6** were obtained by vapour diffusion of CH_3OH into a CH_2Cl_2 solution of **4** and **6**. Crystal measurements were made on a Rigaku TAXIS-IV imaging plate area detector with graphite monochromated Mo-Kα radiation. Indexing was performed from four oscillations that were exposed for 3.3 min. The crystal-to-detector distance was 86.60 mm with the detector at the zero swing position. Readout was performed in the 0.100 mm pixel mode. All calculations were performed using the TEXSAN crystallographic software package of Molecular Structure Corporation.†

Anion complexation studies in solution

The sapphyrin and rubyrins reported here have strong absorption in the visible region and hence we have made use of electronic spectra to monitor the anion complexation. Specifically, a constant volume of sapphyrin or rubyrin in its protonated form in methanol was taken in about ten 10 ml volumetric flasks, and an increasing amount of the required anion salt was added to each flask. Then, in each flask, 1 ml of 0.5 M 18-crown-6 was added, so that the cation was complexed by the crown ether leaving the free anion for binding with the expanded porphyrins. The remaining volume was made up to the mark by the solvent. The solution was shaken well. Addition of salt solution changed the colour of the solution from pink to brown. Immediately

† CCDC reference number 188/257. See http://www.rsc.org/suppdata/p2/b0/b004687f/ for crystallographic files in .cif format.

 DOI: 10.1039/b004687f

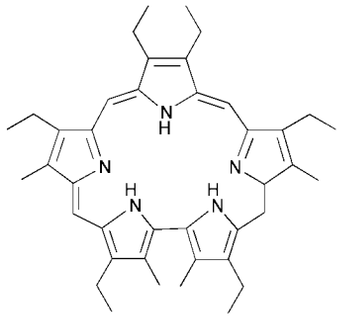

1

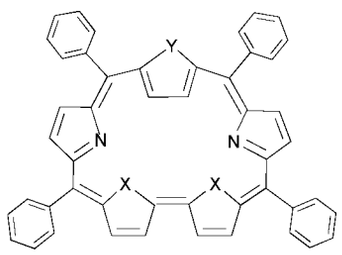

	X	Y
3.	S	O
4.	S	S
5.	S	Se
6.	Se	O

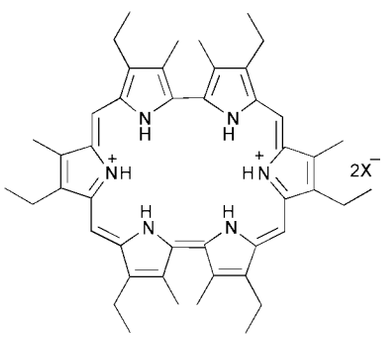

2

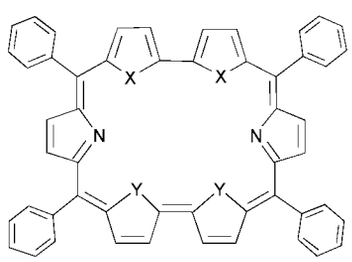

	X	Y
7.	S	O
8.	S	S
9.	Se	O
10.	Se	Se

Scheme 1 Molecular structure of various sapphyrins and rubyrins.

the absorption spectra of these solutions in the desired region were taken in the overlay mode. The addition of an increasing amount of the salt resulted in the gradual decrease of absorbance of protonated macrocycle and a simultaneous blue shift of the absorption band. This decrease in absorption is analysed using the Nash equation[16] to evaluate the binding constants.

$$\frac{1}{C_A} = \left[\frac{d^0}{d^0 - d}\left(K - \frac{\varepsilon_{AD}}{\varepsilon_D}\right) - K\right] \qquad (1)$$

Here d^0 is the optical density of sapphyrin or rubyrin at a particular wavelength in the absence of any salt while d is

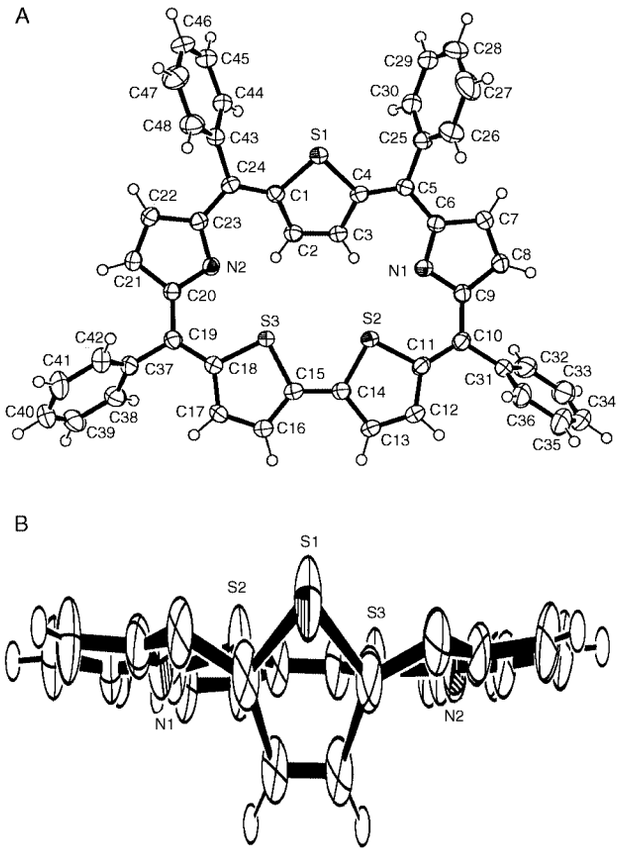

Fig. 1 Single-crystal X-ray structure of **4**: (A) Top view, (B) Side view showing the atomic labelling scheme. The *meso*-aryl rings are deleted for clarity in the side view.

the optical density of the anion complex of the sapphyrin or rubyrin at a particular concentration of the salt solution. C_A is the concentration of the anion, ε_D represents the molar absorptivity of the protonated sapphyrin or rubyrin, while ε_{AD} represents the molar absorptivity of the anion complex of sapphyrin or rubyrin and K is the binding constant. The physical significance of this equation is quite clear when the reciprocal of anion concentration $1/C_A$ is plotted against $d^0/(d^0 - d)$. The intercept of the straight line should be the negative of the binding constant and the slope is related to the molar absorptivity of the complex. This equation is made use of in the present study to evaluate the binding constants. Two to three sets of data were collected for each of the macrocycle interaction with different anions. The straight line plots support the 1 : 1 stoichiometry of the complexes formed.

Results and discussion

Structural analysis of sapphyrins and rubyrins

Unlike, β-substituted sapphyrin **1**, the *meso*-aryl sapphyrins show structural diversity. For example, the β-substituted N5-sapphyrin **1** shows a normal structure where all the pyrrole ring nitrogens are pointing towards the ring current of the macrocycle.[8] On the other hand, the corresponding *meso*-aryl N5-sapphyrin reported by Latos-Grazynski and coworkers show an inverted structure where the pyrrole ring opposite to the bipyrrole unit is inverted in its free base form.[17] Upon protonation, this pyrrole ring experiences a 180° flip to revert back to normal structure.[18] The spectroscopic data for the sapphyrins **3**–**6** reported here suggests that the heterocyclic ring opposite to the bithiophene/biselenophene unit is inverted in its free base form.[14] This ring inversion is further confirmed in the solid state by the single crystal X-ray structure determination of **4** and **6** (Figs. 1 and 2). It is seen from Fig. 1 that the sapphyrin skeleton

Table 1 Selected X-ray structural data for **4** and **6**

Compound	Bond length/Å		Bond angles/°		Non-bonded distances/Å	
4	S2–C11	1.745(4)	C23–C24–C1	121.3(3)	S2 · · · N1	2.667
	C11–C12	1.404(5)	C24–C1–S1	122.8(3)	S2 · · · C3	3.446
	C12–C13	1.381(5)	C24–C1–C2	128(3)	S2 · · · C2	4.011
	C14–C15	1.417(5)	S1–C1–C2	109.1(2)	S2 · · · N2	5.186
	N2–C23	1.353(4)	C1–C2–C3	114.6(3)	S2 · · · S3	3.083
	C22–C23	1.454(4)	C1–S1–C4	93.1(2)		
	C21–C22	1.362(5)				
6	Se1–C1	1.863(6)	C13–C14–C15	119.2(5)	Se1 · · · N2	2.610
	C1–C2	1.404(9)	C14–C15–O	119.5(5)	Se1 · · · C17	3.384
	C2–C3	1.418(8)	C14–C15–C16	133.1(5)	Se1 · · · C16	3.928
	C4–C5	1.418(8)	O–C15–C16	107.4(5)	Se1 · · · N1	5.107
	N1–C13	1.345(8)	C15–C16–C17	108.4(5)	Se1 · · · Se2	3.072
	C12–C13	1.465(8)	C15–O–C18	107.5(5)		
	C11–C12	1.346(9)				

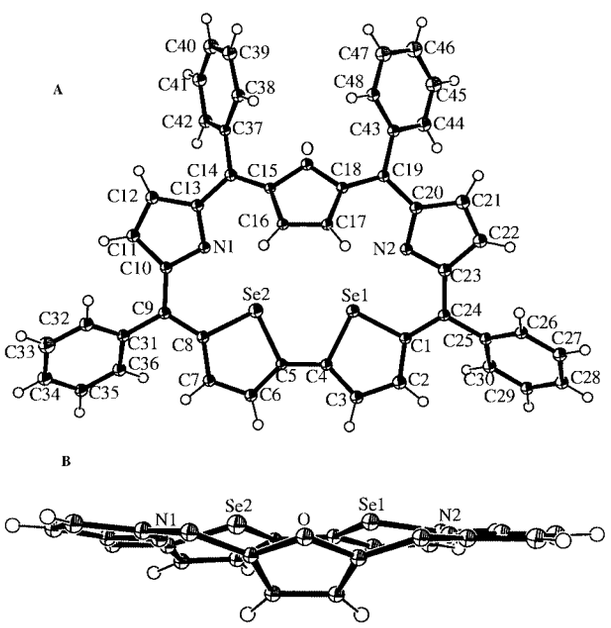

Fig. 2 Single-crystal X-ray structure of **6**: (A) Top view, (B) Side view showing the atomic labelling scheme. The *meso*-aryl rings are deleted for clarity in the side view.

shows a small deviation from planarity; the deviation of the *meso*-carbons for **4** are C(5) 0.0382, C(10) −0.0260, C(19) 0.0265, C(24) −0.0365 Å except for the thiophene ring which is inverted and the sulfur atom is pointing away from the ring current of the macrocycle while the β-CH protons experience the ring current of the macrocycle. The dihedral angle between the inverted thiophene ring and the mean plane of the sapphyrin is 28.28°. For **6** (Fig. 2) the deviations for the *meso*-carbons are C(9) 0.058 (6), C(14) −0.108, C(19) 0.109, C(24) −0.054(6) Å except for the furan ring which is inverted and the oxygen atom is pointing away from the ring current of the macrocycle while the β-CH protons are experiencing the ring current of the macrocycle. The dihedral angle between the furan ring and the mean plane of the sapphyrin is 34.42°.

Table 1 lists the relevant bond lengths, bond angles and the non-bonded distances of **4** and **6**. A comparison of the bond lengths of C_α–X, C_α–C_β and C_β–C_β observed for the heterocyclic ring opposite to the bithiophene and biselenophene unit in **4** and **6** with those of the free heterocyclic ring system suggests small decreases in C_α–X and C_α–C_β distances and small increases in C_β–C_β distances due to the modified aromatic delocalisation pathway in sapphyrins relative to free heterocyclic rings. The bonding pattern in the biselenophene moiety for **6** is reversed if we look at the C_α–C_β and C_β–C_β bond length of the biselenophene units 1.404(9) and 1.418(8) Å respectively, compared to those in a free selenophene ring (1.369 and 1.433 Å). However, the C_α–Se (1.863(6) Å) bond experiences very little change relative to a free selenophene ring (1.855 Å).[19] The crystal data are compiled in Table 2.

Table 2 Crystal data and data collection parameters for **4** and **6**

Parameters	**4**	**6**
Empirical formula	$C_{49}H_{31}N_2S_3Cl_3$	$C_{48}H_{30}ON_2Se_2$
Formula weight	850.34	808.70
Dimensions/mm	0.50 × 0.50 × 0.10	0.25 × 0.18 × 0.03
Crystal system	monoclinic	triclinic
a/Å	12.66(1)	12.638(4)
b/Å	11.36(2)	14.765(13)
c/Å	29.16(2)	10.037(2)
α/°	90	94.34(2)
β/°	95.51(10)	100.79(2)
γ/°	90	108.72(2)
V/Å^3	4174(7)	1724.4(9)
Space group	$P2_1/n$ (#14)	$P\bar{1}$ (#2)
Z value	4	2
μ (MoKα)/cm^{-1}	4.07	21.88
Residuals: R_1	0.074	0.062
Reflections measured	10013	8259
T/°C	−39 ± 1	−131 ± 1

The *meso*-aryl rubyrins also show structural diversity by exhibiting planar and inverted structures.[20] We have recently shown that the adaptation of the planar or the inverted ring depends upon the nature of the heterocyclic ring present as well as the way they have been linked in a cyclic fashion. However, the rubyrins **7**–**10** reported here show a planar structure where all the donor atoms of the heterocyclic rings are pointing towards the ring current of the macrocycle.[15] The β-substituted N6 rubyrins **2** also show a planar structure in the protonated form.[12]

A comparison of the structure of **2** with that of **10** shows some interesting observations.

1. The substitution of the pyrrole by selenophene changes the π-electron delocalization and the bond distances are altered accordingly relative to those observed for the HCl salt of the N6 rubyrins **2**, and the aromatic nature of the macrocycle is evident from the observation that the C_α–C_β distances 1.39(1) Å and 1.40(1) Å are higher than the C_β–C_β distances [1.37(1) Å].[12]

2. A comparison of interpyrrole (heterocycle) angles at the bridging methines with those of **2** reveals significant lowering of these angles. For example; these angles are 124.4° and 125.2° for **10**,[20] while they are 137.0° and 137.63° for **2**.[12] Surprisingly these angles are closer to that observed for protonated form of octaethyl porphyrins (127.0°)[21] suggesting that the lowering of the inner core upon substitution of larger selenium atoms.

3. A decrease in the core size upon the substitution of the larger Se atom, which is reflected in the non-bonded distances

between the Se atoms of 3.468 Å and 4.968 Å for **10**[20] relative to the non-bonded distances between the pyrrole nitrogens which are 5.559 Å and 6.352 Å observed for **2**.[12]

Anion complexes of sapphyrins and rubyrins

Three different anions, F^-, N_3^- and CO_3^{2-}, were chosen to study the complexation with protonated sapphyrins **3**–**6** and protonated rubyrins **7**–**10**. Fig. 3 shows the effect of titration of different concentrations of CO_3^{2-} ion on the absorption spectra of the protonated derivative of **9**. The inset shows the plot of $1/C_A$ *vs.* $d^0/(d^0 - d)$. In a typical experiment, the specific changes occurring upon protonation as well as anion complexation are:

1. Protonation results in a red shift of the Soret band and the magnitude of the red shift varies from 5 to 19 nm.

2. Addition of different amounts of anions to a rubyrin solution of **9** at constant concentration results in a decrease in the absorbance at 550 nm and the simultaneous appearance of a new band at 531 nm. Thus effectively, the anion complexation results in the blue shift of the Soret band[8] of the diprotonated rubyrin and the magnitude of this blue shift is different for different rubyrins. These shifts on going from free base to diprotonated rubyrin to anion complex for different sapphyrins and rubyrins are listed in Table 3.

3. It is seen from Fig. 3 that there are isosbestic points suggesting the presence of an equilibrium between the free diprotonated species and the anion complex. It is pertinent to mention here that the heterocyclic ring opposite to the bithiophene/biselenophene unit remains inverted[14] upon protonation and anion complexation.

A typical characteristic of anion binding of **4** with different anions is shown in Scheme 2. It is seen from Scheme 2 that the protonated **4** binds anions such as F^-, N_3^-, and CO_3^{2-} and the binding constant varies as $F^- \cong N_3^- < CO_3^{2-}$. It has been shown that the binding constant depends on the compatibility of the cavity size of the receptor and the size of the anion and the number of H-bonding sites available.[7] A comparison of binding constants for the fluoride complex of protonated **1** (10^6 M^{-1})[22] relative to **4** reveals a drastic decrease in the binding constant. This decrease is attributed to: 1. The difference in the structures of **1** and **4**. 2. The reduced number of H-bonding

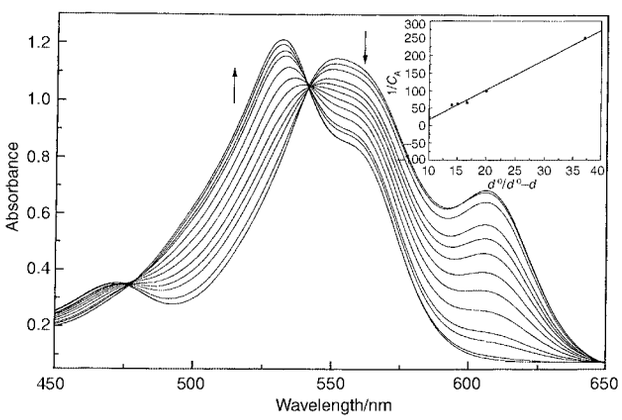

Fig. 3 Effect of CO_3^{2-} ion titration on absorption spectra of protonated **9** in methanol. The inset shows a plot of $1/C_A$ *vs.* $d^0/(d^0 - d)$. The concentration of the Rubyrin used was 1.6×10^{-6} M and the concentration range of the CO_3^{2-} used was 6.90×10^{-4} to 4.14×10^{-3} M. The data shown in the inset were measured at 530 nm at 23 °C.

Table 3 Absorption data for core modified sapphyrins and rubyrins and their receptor complex in the Soret region

	Soret band λ/nm		Anion complex		
Compound	Free base	Diprotonated	F^-	N_3^-	CO_3^{2-}
3	511	519	505	505	504
4	507	512	501	502	502
5	507	519	502	501	502
6	532	539	526	526	525
7	529	536	523	524	522
8	523	538	516	516	616
9	539	550	531	530	530
10	541	560	534	535	533

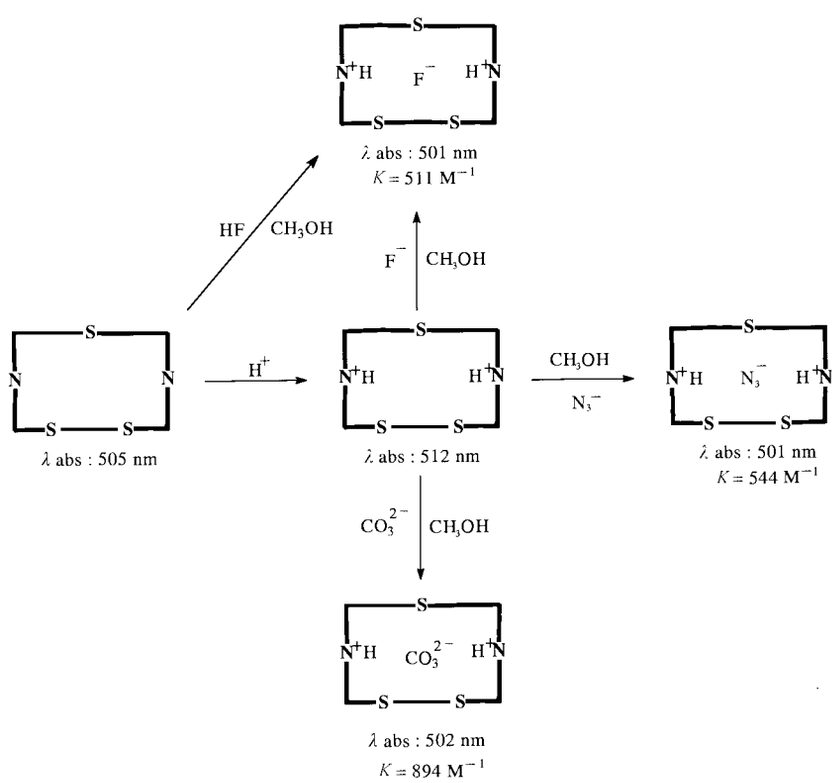

Scheme 2 Characteristics of anion binding of **4**.

Table 4 Concentration range used for various anions (in moles) and the binding constants of the complex with various sapphyrins and rubyrins. The concentrations of sapphyrins and rubyrins were kept constant at ~10^{-6} M

Compound	Concentration range/mol dm^{-3}			Binding constant K/M^{-1} [a]		
	KF	NaN_3	K_2CO_3	KF	NaN_3	K_2CO_3
3	1.43×10^{-4}–2.91×10^{-3}	1.63×10^{-4}–6.50×10^{-3}	6.91×10^{-5}–1.04×10^{-3}	590	821	1182
4	1.45×10^{-3}–5.81×10^{-3}	3.25×10^{-4}–3.25×10^{-3}	2.07×10^{-4}–1.66×10^{-3}	511	544	894
5	2.91×10^{-4}–5.81×10^{-3}	3.25×10^{-4}–1.95×10^{-3}	1.38×10^{-4}–1.38×10^{-3}	172	292	827
6	5.81×10^{-4}–2.91×10^{-3}	6.50×10^{-4}–3.25×10^{-3}	2.76×10^{-4}–2.76×10^{-3}	210	240	734
7	1.45×10^{-3}–2.91×10^{-2}	6.50×10^{-4}–2.60×10^{-2}	1.38×10^{-3}–2.76×10^{-3}	78	896	1372
8	1.63×10^{-3}–3.50×10^{-3}	1.30×10^{-4}–6.50×10^{-3}	1.38×10^{-4}–2.76×10^{-3}	49	767	1290
9	1.45×10^{-3}–1.16×10^{-2}	6.50×10^{-4}–1.30×10^{-2}	6.90×10^{-4}–4.14×10^{-3}	42	374	674
10	5.81×10^{-4}–2.32×10^{-3}	3.25×10^{-4}–1.30×10^{-3}	6.90×10^{-4}–4.14×10^{-3}	29	130	224

[a] The estimated error is ±5%.

sites in **4** (only two sites) relative to **1** (five sites). The larger binding constants observed for CO_3^{2-} relative to the fluoride and azide complexes is in part ascribed to the complete charge neutralisation. This conclusion is supported by the observation from the emission studies where a two hundred-fold increase in the intensity of the emission band was observed for the phosphate and carbonate complexes relative to the fluoride complex.[15a]

The binding constants evaluated and the exact concentration of different anions used for various sapphyrins and rubyrins are tabulated in Table 4. It is seen from Table 4 that the binding constant decreases on going from **3** to **5** for the F^-, N_3^- and CO_3^{2-} complex. This decrease in the binding constant is attributed to the reduced cavity size upon going from **3** to **5**. The X-ray analysis described earlier reveals that the dihedral angle between the inverted ring and the mean sapphyrin plane increases as the size of the heteroatom decreases. For example, the dihedral angle for **4** is 28.28° and for **5**, it is 20.56°.[14b] Similarly, **3** should have a higher dihedral angle compared to **4**. This implies that the cavity size is bigger in **3** relative to **4** and **5**. A comparison of the size of the F^- ion and the cavity size in **3** suggests compatibility between the two sizes and it is anticipated that the binding is more efficient relative to **4** and **5**. On the other hand, N_3^- and CO_3^{2-} ions are larger in size and therefore, it is expected that these two ions are sitting above the plane of the sapphyrins. It is pertinent to point out here that the X-ray crystal structures of F^-, N_3^- and CO_3^{2-} complexes of β-substituted sapphyrin **1** reveal different modes of binding.[22] In the fluoride complex, the F^- ion is sitting at the centre of the cavity of the sapphyrin and is held by five N–H···F hydrogen bonds,[8] while in the azide complex, only one of the terminal nitrogens is involved in the binding and is 1.13 Å above the macrocycle mean plane held by four N1–H···N hydrogen bonds in an end-on fashion.[11] In the case of the benzoic acid complex, the ligated oxygen atom is held at 1.195 Å above the plane of the five pyrrolic nitrogen atoms with five H-bonding interactions.[10a] In contrast to the β-substituted sapphyrins, for the sapphyrins described here, the presence of the heteroatom in the cavity restricts the number of hydrogen bonds to only two, revealing less effective binding with fluoride, azide and carbonate ions relative to **1**. The higher binding constants observed for CO_3^{2-} relative to the azide and fluoride complexes is probably due to the complete charge neutralisation in the CO_3^{2-} as against partial neutralisation by the F^- and N_3^- complexes.

For the diprotonated rubyrins **2**, the binding constant for the fluoride complex decreases drastically relative to the N_3^- and CO_3^{2-} complexes (Table 4). This is probably due to the mismatch of the sizes since the rubyrins have much larger cavities compared to the sapphyrin. For the N_3^- and CO_3^{2-} complexes, there is a decrease in the binding constant on going from **7** to **10**. This can be explained by a gradual decrease of cavity size on going from **7** to **10** because of the substitution of the larger Se atoms. Compared to **2**,[12] the number of H-bonding sites is lower for the rubyrins **7** to **10** because of the presence of heteroatoms.

Conclusion

It can be shown that the protonated core modified sapphyrins and rubyrins bind various anions and the binding constant observed depends upon the cavity size, the number of H-bonding sites and the structure of the macrocycle. Furthermore, **4** and **6** adopt inverted structures where the heterocyclic ring opposite to the bithiophene/biselenophene unit is inverted while the rubyrin **10** shows the planar structure.

Acknowledgements

This work was supported by a grant from the Department of Science and Technology, New Delhi, India to T. K. C. He is also grateful to the Alexander von Humboldt foundation for an equipment grant.

References

1 (*a*) J. L. Sessler and S. J. Weghorn, in *The Porphyrin Handbook*, eds. K. M. Kadish, K. M. Smith and R. Guilard, Academic Press, San Diego, 2000, Vol. 2, pp. 55–124; (*b*) A. Jasat and D. Dolphin, *Chem. Rev.*, 1997, **97**, 2267.
2 (*a*) M. Ravikanth and T. K. Chandrashekar, *Struct. Bonding* (*Berlin*), 1995, **82**, 105; (*b*) R. P. Pandian and T. K. Chandrashekar, *Inorg. Chem.*, 1994, **33**, 3317; (*c*) R. P. Pandian and T. K. Chandrashekar, *J. Chem. Soc.*, *Dalton Trans.*, 1993, 119; (*d*) M. Ravikanth, A. Mishra, T. K. Chandrashekar, S. Sathaiah and H. D. Bist, *Inorg. Chem.*, 1994, **33**, 392.
3 (*a*) J. L. Sessler, G. W. Hemmi, T. D. Mody, T. Murai, A. Burrell and S. W. Young, *Acc. Chem. Res.*, 1994, **27**, 43; (*b*) S. W. Young, K. W. Woodburn, M. Wright, T. D. Mody, Q. Fan, J. L. Sessler, W. C. Dow and R. A. Miller, *Photochem. Photobiol.*, 1996, **63**, 892.
4 J. L. Sessler, T. D. Mody, G. W. Hemmi, V. Lynch, S. W. Young and R. A. Miller, *J. Am. Chem. Soc.*, 1993, **115**, 10368.
5 S. W. Young, F. Qing, A. Harriman, J. L. Sessler, W. C. Dow, T. D. Mody, G. Hemmi, Y. Hao and R. A. Miller, *Proc. Natl. Acad. Sci. U. S. A.*, 1996, **93**, 6610.
6 (*a*) J. L. Sessler, D. A. Ford, M. J. Cyr and H. Furuta, *J. Chem. Soc.*, *Chem. Commun.*, 1991, 1733; (*b*) H. Furuta, K. Furuta and J. L. Sessler, *J. Am. Chem. Soc.*, 1991, **113**, 4707; (*c*) H. Furuta, M. J. Cyr and J. L. Sessler, *J. Am. Chem. Soc.*, 1991, **113**, 6677.
7 J. L. Sessler, A. Andrievsky and J. W. Genge, *Advances in Supramolecular Chemistry*, 1997, **4**, 97.
8 J. L. Sessler, M. J. Cyr, V. Lynch, E. McGhee and J. A. Ibers, *J. Am. Chem. Soc.*, 1990, **112**, 2810.
9 V. Král, H. Furuta, K. Shreder, V. Lynch and J. L. Sessler, *J. Am. Chem. Soc.*, 1996, **118**, 1595.
10 (*a*) J. L. Sessler, A. Andrievsky, V. Král and V. Lynch, *J. Am. Chem. Soc.*, 1997, **119**, 9385; (*b*) J. L. Sessler, M. C. Hoehner, A. Gebauer, A. Andrievsky and V. Lynch, *J. Org. Chem.*, 1997, **62**, 9251.
11 J. L. Sessler, M. J. Cyr and A. K. Burrell, *Synlett*, 1991, 127.

12 J. L. Sessler, T. Morishima and V. Lynch, *Angew. Chem.*, *Int. Ed. Engl.*, 1991, **30**, 977.
13 S. J. Narayanan, B. Sridevi, T. K. Chandrashekar, A. Vij and R. Roy, *J. Am. Chem. Soc.*, 1999, **121**, 9053.
14 (*a*) A. Srinivasan, S. K. Pushpan, M. Ravikumar, S. Mahajan, T. K. Chandrashekar, R. Roy and P. Ramamurthy, *J. Chem. Soc.*, *Perkin Trans. 2*, 1999, 961; (*b*) A. Srinivasan, V. G. Anand, S. J. Narayanan, S. K. Pushpan, M. Ravikumar, T. K. Chandrashekar, K.-I. Sugiura and Y. Sakata, *J. Org. Chem.*, 1999, **64**, 8693.
15 (*a*) A. Srinivasan, M. V. R. Reddy, S. J. Narayanan, B. Sridevi, S. K. Pushpan, M. Ravikumar and T. K. Chandrashekar, *Angew. Chem.*, *Int. Ed. Engl.*, 1997, **36**, 2598; (*b*) A. Srinivasan, S. K. Pushpan, M. Ravikumar, T. K. Chandrashekar and R. Roy, *Tetrahedron*, 1999, **55**, 6671.
16 C. Nash, *J. Phys. Chem.*, 1960, **64**, 950.
17 P. J. Chmielewski, L. Latos-Grazynski and K. Rachlewicz, *Chem. Eur. J.*, 1995, **1**, 68.
18 K. Rachlewicz, N. Sprutta, L. Latos-Grazynski, P. J. Chmielewski and L. Szterenberg, *J. Chem. Soc.*, *Perkin Trans. 2*, 1998, 959.
19 L. Latos-Grazynski, E. Pacholska, P. J. Chmielewski, M. M. Olmstead and A. L. Balch, *Inorg. Chem.*, 1996, **35**, 566.
20 S. J. Narayanan, A. Srinivasan, B. Sridevi, T. K. Chandrashekar, M. O. Senge, K.-I. Sugiura and Y. Sakata, *Eur. J. Org. Chem.*, 2000, 2357.
21 (*a*) E. Cetinkaya, A. W. Johnson, M. F. Lappert, G. M. MacLaughlin and K. W. Muir, *J. Chem. Soc.*, *Dalton Trans.*, 1974, 1236; (*b*) A. Stone and E. B. Fleischer, *J. Am. Chem. Soc.*, 1968, **90**, 2375.
22 M. Shionoya, H. Furuta, V. Lynch, A. Harriman and J. L. Sessler, *J. Am. Chem. Soc.*, 1992, **114**, 5714.